https://doi.org/10.5194/egusphere-2024-3269
Preprint. Discussion started: 4 November 2024

Uncertainties in the effects of organic aerosol coatings on polycyclic aromatic hydrocarbon concentrations and their estimated health effects

Sijia Lou[1,2], Manish Shrivastava[3], Alexandre Albinet[4], Sophie Tomaz[4,5], Deepchandra Srivastava[4,6], Olivier Favez[4], Huizhong Shen[7], Aijun Ding[1,2]

[1]Joint International Research Laboratory of Atmospheric and Earth System Sciences, School of Atmospheric Sciences, Jiangsu Provincial Collaborative Innovation Center of Climate Change, Nanjing University, Nanjing, 210023, China

[2]Frontiers Science Center for Critical Earth Material Cycling, Nanjing University, Nanjing 210023, China

[3]Pacific Northwest National Laboratory, Richland, WA 99354, USA

[4]Institut Nationala de l'Environnement industriel et des RISques (Ineris), 60550, Verneuil en Halatte, France

[5]now at : INRS, 1 rue du Morvan CS 60027, 54519, Vandoeuvre-lès-Nancy, France

[6]now at: School of Geography Earth and Environmental Science, University of Birmingham, Edgbaston, Birmingham, UK B15 2TT

[7]Shenzhen Key Laboratory of Precision Measurement and Early Warning Technology for Urban Environmental Health Risks, School of Environmental Science and Engineering, Southern University of Science and Technology, Shenzhen 518055, China

Correspondence to: Sijia Lou (lousijia@nju.edu.com); Manish Shrivastava (ManishKumar.Shrivastava@pnnl.gov)

https://doi.org/10.5194/egusphere-2024-3269
Preprint. Discussion started: 4 November 2024

Abstract.

We utilized the CAM5 model to examine how different degradation approaches for particle-bound Polycyclic Aromatic Hydrocarbons (PAHs) affect the spatial distribution of benzo(a)pyrene (BaP). Three approaches were evaluated: NOA (no OA coatings), Shielded (where viscous OA coatings protect PAHs from oxidation), and ROI-T (where OA coatings influence PAHs through reactive oxygen intermediates related to temperature). Our findings indicate that the seasonal variation of BaP is influenced by emissions, deposition, and degradation approaches. All simulations predict higher population-weighted global average (PWGA) fresh BaP concentrations during December-January-February (DJF) compared to June-July-August (JJA), primarily due to increased emissions from household activities, less efficient wet removal, and unfavourable winter conditions. The Shielded and ROI-T approaches show that viscous OA coatings significantly inhibit BaP oxidation, leading to PWGA fresh BaP concentrations two to six times higher in DJF than in NOA. The Shielded approach predicts the highest PWGA fresh BaP concentration of 1.3 ng m^{-3} in DJF, with 90% of BaP protected from oxidation. In contrast, the ROI-T approach forecasts lower concentrations in mid-to-low latitudes. Model evaluations indicate the Shielded method performs best, with a normalized mean bias within ±20%. The incremental lifetime cancer risk ranges from 0.6 to 2 deaths per 100,000 persons based on fresh BaP exposure. Overall, the human health risks from fresh and oxidized PAHs are comparable, underscoring the importance of including both forms in risk assessments and highlighting the critical role of accurate degradation approaches in PAH modelling.

https://doi.org/10.5194/egusphere-2024-3269
Preprint. Discussion started: 4 November 2024

1 Introduction

Polycyclic aromatic hydrocarbons (PAHs), emitted from incomplete combustion of biofuels and fossil fuels, are persistent organic pollutants composed of multiple aromatic rings. Some of them are contaminants of global concern due to their well-known carcinogenic and mutagenic properties, which increase the risk to human health [Boffetta et al., 1997; Perera, 1997; Chen and Liao, 2006; IARC, 2010; Kim et al., 2013; Muir et al., 2019]. For instance, in 1976, the United States Environmental Protection Agency (US EPA) listed 16 PAHs as priority pollutants [Keith 2015]. Among these, particle-bound PAHs are more carcinogenic than gas-phase PAHs [Y Liu et al., 2017]. Therefore, benzo(a)pyrene, one of the most carcinogenic PAHs and predominantly existing in the particle phase, is often used as an indicator of cancer risk resulting from exposure to PAH mixtures [EPA 2004; EPCEU 2004; MEPPRC 2009; CPCB, 2020; IARC, 2021]. Considering that lifetime exposure to 0.1 ng m^{-3} of BaP would increase the additional lung cancer risk by one in 100,000 exposed persons, the World Health Organization (WHO) recommends limiting BaP concentrations to 0.1 ng m^{-3} [WHO, 2000; Bostrom et al., 2002].

High levels of BaP in ambient air have been measured globally over the past two decades, ranging from 0.1 to 2.5 ng m^{-3} in Europe and North America, with even higher concentrations observed in rural areas of China and India, exceeding 10 ng m^{-3} [Lee et al., 2011; W Wang et al., 2011; Kim et al., 2012; Brown et al., 2013; Hu et al., 2017; Radonić et al., 2017; Hu et al., 2018; Ma et al., 2018; J Han et al., 2019; Lhotka et al., 2019; Munyeza et al., 2019; Ahad et al., 2020; Kumar et al., 2020]. However, compared to measurements, previous regional or global models suffer from large uncertainties, with biases spanning several orders of magnitude, largely due to an incomplete understanding of the complex gas-particle partitioning [Friedman et al., 2014; Galarneau et al., 2014; Lammel et al., 2015; Shrivastava et al., 2017; Mu et al., 2018; F Han et al., 2022]. For example, Iakovides et al. (2021) reported that using an octanol-air partition coefficient absorption model, such as the Junge-Pankow model, the gas-particle fractions of simulated PAHs are more suitable for remote or rural areas but not for urban areas. To differentiate between aerosols in European urban or rural areas, Arp et al. (2008) developed polyparameter linear free energy relationships (ppLFER) equations. Shahpoury et al. (2016) reported that the ppLFER model can distinguish a variety of organics, including liquid water-soluble/organic soluble organics, and solid/semisolid organic polymers, as well as the inorganic phases of aerosols. Therefore, by adopting the ppLFER scheme, the gas-particle partitioning of simulated PAHs in anthropogenically impacted areas is improved, and the simulated PAHs show good agreement with observations [Tomaz et al., 2016; Kelly et al., 2021].

The lack of clarity regarding the chemical loss of PAHs is a significant factor contributing to large deviations in model-simulated BaP concentrations compared to measured values. As a semi-volatile compound, BaP in the gas-phase undergoes degradation through various pathways, primarily involving reactions with OH and NO_3 radicals, along with photolytic processes driven by light. In a particle-bound state, while BaP can also be degraded by OH and NO_3, this occurs at a much slower rate compared to degradation by ozone, which serves as the primary mechanism in this phase [Keyte et al., 2013]. Laboratory studies have shown that particle-bound BaP can undergo rapid oxidation within hours through heterogeneous chemical degradation of BaP on the surface of black carbon (BC), organic carbon (OC), and sulfate aerosols [Pöschl et al., 2001; Kwamena et al., 2004; Kahan et al., 2006; Zhou et al., 2012]. Despite laboratory findings, field measurements have revealed that BaP persists in the atmosphere for extended periods and can be transported over long distances, reaching even the Arctic [Halsall et al.,

https://doi.org/10.5194/egusphere-2024-3269
Preprint. Discussion started: 4 November 2024

1997; Masclet et al., 2000; Schauer et al., 2003; Lohmann and Lammel, 2004; Van Overmeiren et al., 2024]. A recent laboratory study demonstrated that the presence of secondary organic aerosol (SOA) coatings could shield BaP from ozone oxidation [Zelenyuk et al., 2012]. Based on this, Friedman et al. (2014) used an exponential decay function, assuming that 80% of SOA-bound PAHs were still present after 24 hours. However, the shielding effectiveness of PAHs depends on the phase state of SOA, which should be temperature- and relative humidity-dependent [Koop et al., 2011; Zhou et al., 2013; Berkemeier et al., 2016; Shiraiwa et al., 2017; Shrivastava et al., 2017; Mu et al., 2018]. Shrivastava et al. (2017) developed a new PAH modeling approach in the global Community Atmosphere Model, assuming that viscous SOA can completely inhibit particle-bound PAHs (i.e., BaP) oxidation reactions under cool or dry conditions. Implementing this approach significantly improved the agreement between simulated and measured BaP concentrations at hundreds of locations worldwide compared to models that ignored the shielding effects of SOA coatings. Meanwhile, Mu et al. (2018) suggested that shutting off particle-bound BaP degradation based on the simple thresholds of temperature and relative humidity used in Shrivastava et al. (2017) cannot represent the complex multiphase reactions of BaP. They proposed a new ROI-T approach, accounting for the effects of temperature and humidity on SOA phase state and BaP degradation chemical reaction rate. The BaP concentrations simulated using the ROI-T approach exhibited the best agreement with measurements at Xianghe (China) and Gosan (South Korea) sites [Mu et al., 2018]. However, their simulations still showed a significant underestimation of BaP concentrations for European and Arctic background sites.

Therefore, the oxidation chemistry of particle-bound BaP, highly dependent on the concentrations of oxidants (primarily ozone) and the effectiveness of organic aerosol (OA) coatings, which are influenced by temperature and relative humidity (RH). This dependence results in notable seasonal variations in both fresh BaP concentrations and oxidized BaP. Considering that assessments of PAH-induced lung cancer risks often rely on modeled BaP concentrations [Shen et al., 2014; Shrivastava et al., 2017; F Han et al., 2020; Famiyeh et al., 2021; F Han et al., 2022; Li et al., 2022], uncertainties in modeled BaP concentrations carry significant implications for estimates of PAH exposure and human health risks. This study systematically investigates the uncertainty in simulated BaP concentrations due to varying chemical mechanisms of BaP oxidation across different seasons and evaluates the appropriateness of PAH modeling. This paper is organized as follows: Section 2 introduces the model, particle-bound BaP degradation approaches, emissions, and observation data used in this study. Section 3 first presents the simulated fresh and oxidized BaP concentrations in winter and summer, followed by a detailed comparison between simulated BaP and measurements. Section 4 gives the conclusions and implications for discussions.

2 Methods

2.1 Measurements

We collected observed fresh BaP concentrations at 66 background/remote sites and 208 non-background sites worldwide (Table S1, S2). The observation data of fresh BaP were obtained from the Integrated Atmospheric Deposition Network (IADN, available from https://www.epa.gov/great-lakes-monitoring/great-lakes-integrated-atmospheric-deposition-network), the European Monitoring and Evaluation Programme (EMEP, available from https://www.emep.int [Tørseth et al., 2012]), the Global

https://doi.org/10.5194/egusphere-2024-3269
Preprint. Discussion started: 4 November 2024

Environmental Assessment Information System (GENASIS, available from https://www.genasis.cz), the Arctic Monitoring and Assessment Programme (AMAP [Hung et al., 2010]), and previous studies [Shen et al., 2014; Shrivastava et al., 2017]. For oxidized BaP, measurements were available from only two locations: Grenoble—an urban site situated at 5.73°E, 45.16°N—in 2013, and SIRTA—a background site located at 2.15°E, 48.71°N (http://sirtaa.ipsl.fr/)—in the years 2014-2015. However, due to the measurement limitations, data on oxidized BaP (primarily nitro-BaP) were only available from two sites in France. Therefore, this study only includes concentrations of oxidized BaP from Grenoble (an urban site located at 5.73E, 45.16ºN) in 2013 [Tomaz et al., 2016] and from the ACTRIS SIRTA atmospheric supersite (Site Instrumental de Recherche par Télédétection Atmosphérique, whici is representative of the suburban background conditions in the Paris region, located at 2.15°E, 48.71°N; http://sirtaa.ipsl.fr/) in 2014-2015 [Lanzafame et al., 2021].

2.2 Overview of the model

We employed the global Community Atmosphere Model version 5.2 (CAM5) to simulate the global distribution of BaP concentrations. Tracer concentrations obtained from CAM5 simulations were performed at a horizontal resolution of 1.9 º latitude by 2.5 º longitude, and a vertical resolution of 30 layers between the surface and 3.6 hPa. The Model for Ozone and Related Chemical Tracers (MOZART-4) represented the gas-phase chemical mechanism [Emmons et al., 2010], while the properties and processes of aerosol species were included in the Modal Aerosol Model (MAM3) [X Liu et al., 2012]. The model encompassed six aerosol species, including inorganic aerosols (e.g. mineral dust, black carbon, sulfate, and sea salt) and organic aerosols (primary organic aerosol and secondary organic aerosol). In addition, this study utilized an update of the volatility basis-set (VBS) approach developed by Shrivastava et al. (2015). The VBS approach tracked SOA formation based on SOA precursor gas sources, addressing both functionalization and fragmentation reactions during multi-generational aging of SOA precursor gases, as well as oligomerization reactions of SOA. The ppLFER (polyparameter linear free energy relationships) model was applied to the gas-particle partitioning of BaP, encompassing both BaP absorption into organic aerosols and adsorption onto the surface of black carbon aerosol [Shahpoury et al., 2016]. Following Shrivastava et al. (2017), we divided organic aerosols (OA) into the liquid water-soluble/organic soluble phase and the solid/semi-solid organic polymer phase. More than 90% of particle-bound BaP is absorbed within organic aerosols after applying the ppLFER model. The transport, dry deposition, and wet removal of particle-bound BaP (including oxidized PAH) are treated similarly to other aerosol species in CAM5 [X Liu et al., 2012].

2.3 BaP degradation

The model incorporates the gas-phase reaction of BaP with hydroxyl radicals (OH). Consistent with previous studies, the second-order rate coefficient for the reaction of gaseous BaP with OH is set at 5×10^{-11} cm^3 $molecules^{-1}$ s^{-1} [Keyte et al., 2013; Shrivastava et al., 2017]. Heterogeneous reactions of particulate-phase BaP with OH and ozone are also included in the model [Cazaunau et al., 2010; Zhou et al., 2012; Keyte et al., 2013; Zhou et al., 2013]. The second-order rate coefficient for the reaction of particle-bound BaP with OH is determined to be 2.9×10^{-13} cm^3 $molecules^{-1}$ s^{-1} [Esteve et al., 2006], which is two orders of magnitude slower than the gas-phase reaction rate of BaP with OH. Conversely, particle-bound BaP reacts rapidly with ozone within a few hours, representing the primary oxidation

https://doi.org/10.5194/egusphere-2024-3269
Preprint. Discussion started: 4 November 2024

pathway for BaP. Note that the photolysis of BaP is not included in this study, partly because its photolysis rate constant is much lower compared to that of low molecular wight PAHs [Niu et al., 2007], and the current model already underestimates BaP concentrations.

In this study, three approaches are implemented to estimate particle-bound BaP degradation, providing insights into the uncertainty associated with this process.

(1) In the default NOA approach, the organic coating does not affect the BaP heterogeneous loss process. The heterogeneous oxidation of particle-bound BaP follows the Langmuir-Hinselwood mechanism, indicating that the first-order reaction rate (k) is variable dependent on ozone concentrations, without diffusion limitations from thin liquid-like SOA coatings [Zhou et al., 2012; Zhou et al., 2013].

(2) Following Shrivastava et al. (2017), the SOA Shielded approach is implemented, accounting for the shielding of BaP by viscous SOA coatings. The kinetics of the heterogeneous oxidation of BaP with ozone become much slower after absorption by organic aerosols, as thick OA coatings reduce the kinetics of mass transfer of BaP from the interior of the particle to the particle surface. The effectiveness of SOA shielding is related to its thickness and viscosity, influenced by temperature and relative humidity [Zhou et al., 2012; Zhou et al., 2013]. In this approach, when SOA coatings are less than 20 nm, we assume that SOA cannot effectively shield particle-bound BaP, and thus, the heterogeneous oxidation kinetics remain the same as in the default NOA approach. Thick SOA coatings (> 20 nm) can completely turn off the particle-bound BaP heterogeneous loss kinetics under dry or cool conditions (relative humidity < 50% or temperature < 296 K). Different oxidation kinetics with ozone are applied under humid and warm conditions with thick SOA coatings, where the second-order rate coefficient for the reaction of particle-bound BaP with ozone is 14 and 6.2×10-15 cm3 molecules-1 s-1 under moderate humidity (50%≤RH<70%) and high humidity conditions (RH≥70%), respectively [Zhou et al., 2013; Shrivastava et al., 2017].

(3) Following Mu et al. (2018), the ROI-T approach is implemented, accounting for the temperature and humidity dependence of the phase state, diffusivity, and reactivity of particulate-phase BaP. First-order reaction rate coefficients for BaP ozonolysis are sensitive to both temperature and RH below room temperature (296 K), but are only temperature sensitive above room temperature [Mu et al., 2018]. Under cool and dry conditions, the first-order reaction rate coefficients are four orders of magnitude lower than those under warm conditions. Notably, the ROI-T approach yields a much slower oxidation reaction of particle-bound BaP than the default NOA approach under cool and dry conditions but a faster oxidation reaction rate under warm conditions.

2.4 Model Sensitivity Simulations

We conduct simulations using CAM5 to explore the uncertainty of seasonal variations in BaP concentrations with different PAH oxidation approaches. Three effects of OA coatings on particle-bound PAH oxidation, as detailed in section 2.3, are considered. Hence, sensitivity simulations are performed as follows:

(1) NOA (OA coatings do not affect PAH oxidation);

(2) Shielded (viscous OA coatings turning off BaP reaction with ozone under cool and dry conditions) [Shrivastava et al., 2017];

https://doi.org/10.5194/egusphere-2024-3269
Preprint. Discussion started: 4 November 2024

(3) ROI-T (the reaction rate between BaP and ozone varies with the effectiveness of OA coatings based on temperature and RH) [Mu et al., 2018].

All simulations are conducted over two years, with the first year allocated for spin-up. Since most observations occurred around 2004-2009, winds and temperature are nudged toward ERA-Interim data from January 2007 to December 2008 in this study.

2.5 Emissions

This study utilizes the Global Emission Modeling System (GEMS) 0.1º × 0.1º global BaP emission inventory with temporal and spatial variations, which is available from gems.sustech.edu.cn. The inventory includes data from all major fuel consumption sources and industrial processes [Shen et al., 2013]. The spatiotemporal changes in global BaP emissions are detailed in our previous work [Shrivastava et al., 2017; Lou et al., 2023]. Anthropogenic emissions, including BC, OC, and precursor gases for both secondary aerosols and ozone, are sourced from the HTAP_v2.2 2008 emission inventory [Janssens-Maenhout et al., 2015]. Additionally, emissions from agricultural waste burning and open biomass burning emissions are obtained from the Emissions Database for Global Atmospheric Research (EDGAR v4.3) and Global Fire Emissions Database (GFED3.0), respectively [van der Werf et al., 2010; Crippa et al., 2018]. To maintain consistency with the modeling timeframe and facilitate comparison with observations, all emissions are set at 2008 levels.

2.6 Global model downscaling formulation

To enhance the comparison between simulated BaP concentrations and measurements, particularly in anthropogenically influenced sites such as those near cities, we implemented downscaling. This involved reducing the model-calculated near-surface BaP concentrations from the coarse grid resolution of 2.5°×1.9° to a higher resolution (0.1°×0.1°). Following the methodology outlined by Shen et al. (2014), we assigned a weighting factor (W_i) for each 0.1°×0.1° receiving grid. This factor was determined by summing the contributions of emissions from all 0.1°×0.1° emission grids within a nine-grid neighborhood (one 2.5°×1.9° grid covering the 0.1°×0.1° receiving grid and the other eight surrounding it). The formulation for W_i is as follows:

$$W_i = \sum_{j=1}^{n} \frac{2.03 Q_j f_j e^{-r_d t_{ji}}}{u_j \sigma_{z_j} x_{ji}} \qquad (1)$$

Here, Q_j (ng/s) represents the emissions density of the jth emission grid. f_j (dimensionless) and u_j (m/s) are wind frequency (0-1) and wind speed in directions 1 to 16 in the jth emission grid, respectively, taken from the ERA-interim reanalysis wind field. The degradation rate r_d (/s) involves the gas-phase reaction with OH and the particle-phase heterogeneous reaction with ozone in the receiving grid based on simulation output. Additionally, t_{ji} (s) and x_{ji} (m) denote the distance and transport time from the jth emission grid to the ith receiving grid, and σ (m) is the vertical standard deviation of the concentrations. Finally, the calculated W_i is used as a proxy to disaggregate the model-calculated concentration of each 2.5°×1.9° model grid to a 0.1°×0.1° grid. Previous studies have reported substantial improvements in the distribution and magnitude of observed BaP concentrations through this downscaling process in similar simulations [Shen et al., 2014; Shrivastava et al., 2017; Lou et al., 2023].

https://doi.org/10.5194/egusphere-2024-3269
Preprint. Discussion started: 4 November 2024

2.7 Incremental Lifetime Cancer Risk

The Incremental Lifetime Cancer Risk (ILCR) induced by exposure to PAHs in ambient air is calculated using the following formula [Shen et al., 2014]:

$$ILCR = CSF \times LADD \times SUS = CSF \times \frac{C \times IR \times y}{BW \times LE} \times SUS \quad (2)$$

where CSF, LADD, and SUS represent the cancer slope factor, lifetime average daily dose, and a factor describing individual susceptibility, respectively, depending on age, gender, ethnicity, and geographic region. LADD is calculated from BaP exposure concentration (C, mg m^{-3}), which is downscaled from model-predicted BaP concentrations in this study, inhalation rate (IR, m^3/day), exposure duration (y, year), body weight (BW), and average life expectancy of the global population (LE, 70 years). ILCR in this study is a population-weighted average and represents the maximum likelihood estimate; the unit for ILCR is one death per 100,000 persons.

3 Results

3.1 Simulation of seasonal variations in global fresh BaP

Given that lifetime exposure to 0.1 ng m^{-3} of BaP theoretically results in an additional lung cancer death per 100,000 exposed persons, the WHO recommends a limit of 0.1 ng m^{-3} [Bostrom et al., 2002]. BaP degradation approaches can significantly impact BaP concentrations, further influencing the assessment of PAH exposure risks in various regions. Here, in this study, we investigated three different particle-bound BaP degradation approaches related to the OA coating hypothesis to examine their effects on the spatial distribution of BaP. Considering that the effectiveness of OA coatings is strongly dependent on temperature and humidity variations, we analyzed the distribution of BaP concentrations under different seasons.

In DJF (December-January-February), population-weighted global average (PWGA) BaP concentrations with different particle-bound BaP degradation approaches are predicted to be 0.24-1.38 ng m^{-3}, consistently exceeding the WHO recommendation. High levels of BaP concentrations are simulated to appear in East Asia, South Asia, North Africa, and Europe, with the peak BaP exposure in eastern China exceeding 1.0 ng m^{-3} (Fig. 1). In contrast, BaP concentrations are much lower in JJA (June-July-August), with population-weighted global average values of 0.04-0.17 ng m^{-3}. These results indicate that the simulated BaP exhibits strong seasonality, primarily influenced by changes in emissions, deposition, and BaP degradation chemistry. In 2008, residential biomass use contributed more than 60% of total atmospheric BaP emissions for households cooking, heating, and lighting [Shen et al., 2013]. Since the demand for heating and lightning is higher in winter than in summer, more residential biomass burning is required in winter, inevitably producing BaP. In addition, less precipitation in the Northern Hemisphere in winter compared to summer (Fig. S1), linked to less efficient wet removal, contributes to the seasonal variations of BaP. Thus, without the impacts of OA coatings on BaP degradation, the seasonal variations of BaP concentrations in simulations using the NOA approach primarily represent the changes in emissions and deposition.

https://doi.org/10.5194/egusphere-2024-3269
Preprint. Discussion started: 4 November 2024

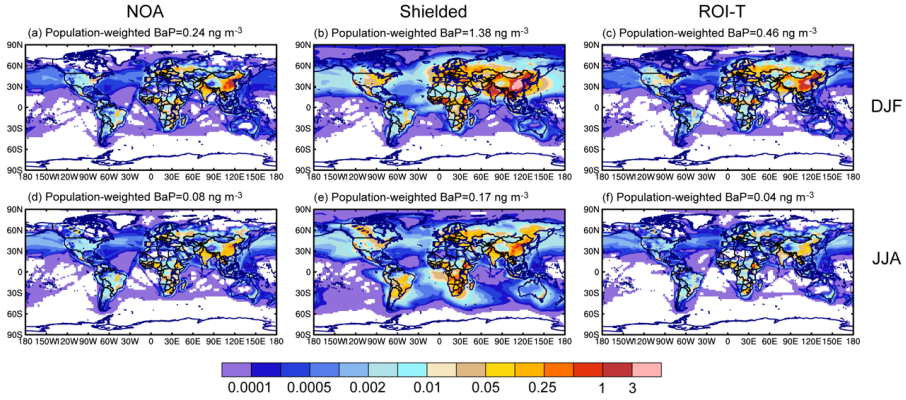

Figure 1. The spatial distribution of simulated BaP concentrations in (a-c) DJF and (d-f) JJA. Fresh BaP concentrations with different heterogeneous reaction approaches for particle-bound BaP are shown in the left column (NOA), the middle column (Shieled), and the right column (ROI-T), respectively.

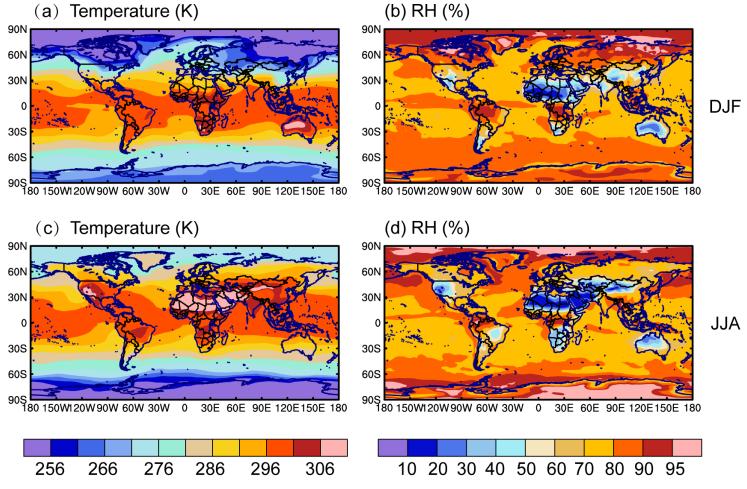

Figure 2. The spatial distribution of surface-layer average temperature (left column, unit: K) and relative humidity (right column, unit: %) in DJF (December-January-February) and JJA (June-July-August), respectively.

Compared with simulations using the NOA approach, those incorporating OA coatings can effectively impede the BaP loss process, leading to a significant increase in BaP concentrations during winter (Fig. 1). Upon absorption by organic aerosols, the presence of viscous OA coatings substantially hinders the mass transfer kinetics of BaP from the particle core to the surface. The denser the organic aerosol, the slower the diffusion of BaP, consequently slowing down the heterogeneous reactions of particle-bound BaP with ozone and OH on the aerosol surface. This effect is more pronounced in winter than in summer, attributed to cooler conditions that likely increase the viscosity of SOA [Shrivastava et al., 2017].

https://doi.org/10.5194/egusphere-2024-3269
Preprint. Discussion started: 4 November 2024

For example, the PWGA BaP from the simulation using the Shielded approach is six times higher than that in the simulation using the NOA approach in DJF. With the Shielded approach, the OA coating is assumed to be sufficiently tacky to prevent BaP from undergoing heterogeneous reactions with ozone completely under dry or cool conditions, thereby extending the lifetime of BaP. During Northern Hemisphere winters, effective OA shielding occurs in areas characterized by cool temperatures (<296 K) or dry conditions (RH<50%), covering most of the regions with high BaP emission densities [Shiraiwa et al., 2011; Saukko et al., 2012; Zhou et al., 2012; Bateman et al., 2015]. Furthermore, BaP with OA coatings can be transported over long distances to remote areas, including the Arctic. Treating OA coating effectiveness as the ROI-T approach, the BaP concentrations also increase, with PWGA BaP estimated to be twice as high as in the simulation with the NOA approach during winter. Compared with the Shielded simulation, BaP concentrations in the ROI-T simulation exhibit similar spatial patterns in high latitudes such as Europe, northern China, and the Arctic, but lower concentrations in southern China, South Asia, and North Africa. The ROI-T approach assumes that the diffusion coefficients of BaP and ozone within OA coatings decrease with reducing temperature and relative humidity, thus reducing the degradation rate of BaP. That is, under cold (<273 K) or dry (<50%) conditions, such as mid-to-high latitudes in winter (Fig. 2a, b), the degradation rates of BaP in the ROI-T approach are two to four orders of magnitude smaller than those without the OA coating effect. In contrast, the OA coating in southern China, South Asia and Africa is not as effective as those in Europe, northern China, and the Arctic, resulting in BaP concentrations similar to NOA simulation.

In JJA, BaP concentrations tend to concentrate near the source areas. While BaP concentrations in the simulation using the Shielded approach are estimated to be higher than those in the NOA simulation, the concentrations found in the simulation using the ROI-T approach are even lower. The ROI-T approach assumes that the diffusion coefficients of BaP and ozone increase with temperature, leading to an estimated faster degradation rate of BaP than in NOA and Shielded approach simulations at conditions above room temperature. Our results are consistent with previous studies [Shrivastava et al., 2017; Mu et al., 2018].

3.2 Simulation of seasonal variations in global oxidized BaP

Previous modeling studies assumed that fresh PAHs are completely degraded after oxidation [Sehili and Lammel, 2007; Matthias et al., 2009; Friedman et al., 2014]. However, laboratory experiments suggested that several oxidized PAHs may remain particle-bound and even increase in molecular weight [Ringuet et al., 2012; Zelenyuk et al., 2012; Jariyasopit et al., 2014]. Furthermore, not only fresh BaP but also certain oxidized BaP species and derivatives exhibit toxicity [EHC 2003; Clergé et al., 2019; Hrdina et al., 2022; Peng et al., 2023]. Therefore, it is essential to understand the impact of different BaP degradation approaches on oxidized BaP.

In this study, we tracked oxidized particle-bound BaP, which is formed through the heterogeneous reactions of particulate-phase BaP with OH and ozone. Figure 3 shows the spatial distribution of simulated oxidized BaP concentrations in DJF. In the absence of an OA coating, particle-bound BaP is always available to react with O_3. Therefore, most particle-bound BaP is rapidly oxidized near source areas, with a PWGA oxidized BaP concentration of 1.3 ng m^{-3}, or 82% of the total (sum of fresh and oxidized) BaP (Fig. 3a, d). If oxidized BaP is as toxic as fresh BaP, the oxidized BaP concentration in NOA globally exceeds the WHO recommendation of 0.1 ng m^{-3} by a wide margin. In comparison, the

https://doi.org/10.5194/egusphere-2024-3269
Preprint. Discussion started: 4 November 2024

Shielded simulation predicts that high levels of oxidized BaP only appear in the tropics in winter (Fig. 3b), because OA coatings are less effective at protecting BaP from ozone attack under high temperature and high RH conditions (Fig. 2a, b). Since the viscous OA coatings completely shut down the particle-bound BaP oxidation reaction under cool or dry conditions, most fresh BaP can stay in the atmosphere for several days, with only 10% of the total BaP being oxidized. Surprisingly, although the OA coating slowed the diffusion of particle-bound BaP from inside the interior of the OA to the particle surface in the ROI-T simulation, 71% of the total BaP was still oxidized on a global basis.

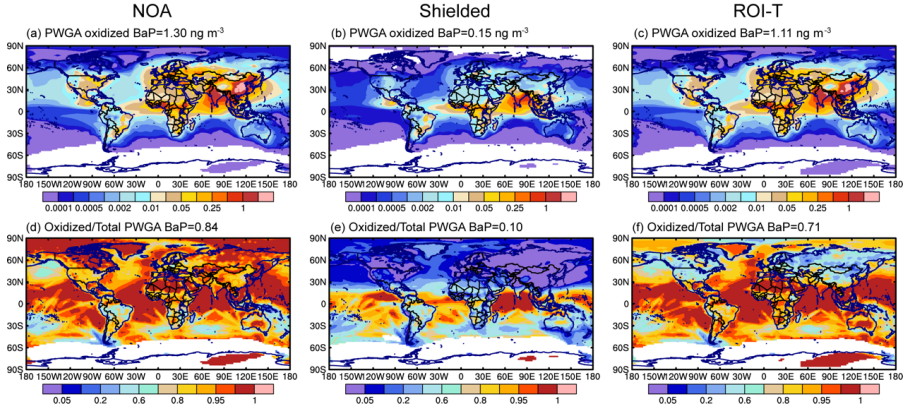

Figure 3. The spatial distribution of simulated (a-c) oxidized BaP concentrations and (d-f) the ratio of oxidized BaP to the total (fresh+oxidized) BaP in DJF. Simulations with the different heterogeneous reactions of particle-bound BaP approaches are shown in the left (NOA simulation), middle (Shield), and right (ROI-T) columns, respectively.

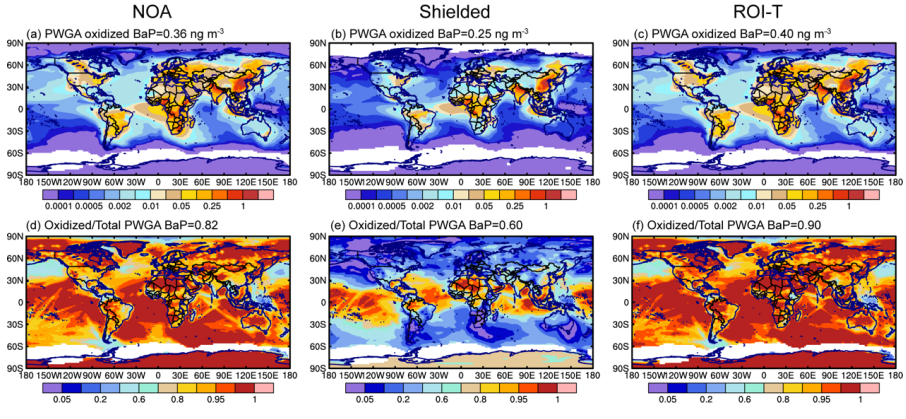

Figure 4. Same as Figure 3 but for JJA.

Due to the less effectiveness of OA coatings under warm and moist conditions, all simulations with different BaP degradation approaches predict that oxidized BaP contributes to more than 90% of the total

https://doi.org/10.5194/egusphere-2024-3269
Preprint. Discussion started: 4 November 2024

BaP concentrations in JJA in the tropics (30°S-30°N). At mid-to-high latitudes, the oxidized BaP varies greatly with the effect of OA coatings on the BaP oxidation reactions. More than 80% of total BaP is oxidized in mid-to-high latitudes applying the NOA or ROI-T approaches, with peaks exceeding WHO recommendations in most of East Asia, West Europe, and North America. Meanwhile, the Shielded approach assumes that OA coatings largely limit the particle-bound BaP oxidation reaction, whereas the oxidized BaP contributes no more than 40% to the total BaP. Our results indicate that current model estimates of human exposure to fresh or oxidized PAHs are highly sensitive to assumptions about PAH degradation processing, especially during North Hemisphere winter.

3.3. Model Evaluation

3.3.1 Fresh BaP

To assess simulated BaP concentrations, we select surface BaP measurements from 66 background/remote sites and 208 urban-affected sites worldwide (Table S1, S2), covering the period 1997 to 2014, with a focus on the years between 2004 and 2011. Median BaP observations at each site are compared with simulated BaP in DJF and JJA, respectively. Given the global model's horizontal grid spacing of approximately 200 km, we specifically compare simulated BaP concentrations with measurements from background sites. To address the limitations of the coarse global model, we downscale the simulated BaP grid to a higher resolution of 10 km based on factors such as wind speed, wind direction and frequency, emission density, and gas/particle BaP degradation rates to account for strong gradients and high BaP concentrations near urban areas. This downscaled approach aims to account for strong gradients and high BaP concentrations near source areas. Our previous studies reported that while the coarse-grid model significantly underestimates concentrations in urban-affected regions, the downscaled BaP vastly improves the comparison between the model and observations [Shrivastava et al., 2017; Lou et al., 2023].

Figure 5a compares measured and model-predicted concentrations at 66 background sites around the world in DJF. The model-estimated BaP for the Shielded approach during the same time and locations of the measurements agrees best with observations of global BaP concentrations, with a normalized mean bias (NMB) of -18%. In contrast, without the effect of OA coating on the degradation of particle-bound BaP, NOA predictions are 78% lower than observed BaP globally (Fig. 5b). Comparisons between measured and downscaled simulated BaP at urban-affected sites show similar results, as the OA shielding approach significantly improves the model's ability to predict fresh BaP concentrations.

It's worth noting that the effectiveness of OA coatings depends largely on temperature and humidity, which are related to the meteorological characteristics of different regions. We, therefore, compare measured and model-simulated BaP concentrations at different latitudes, namely relatively high latitudes (measured locations north of 40°N) and low latitudes (measured locations between 40°S and 40°N), respectively. Figures 6a and 6b demonstrate that the OA shielding particle-bound BaP approach increases the simulated BaP concentrations in much better agreement with the measured values than without the OA coating effect. This improvement is not sensitive to latitude. For the ROI-T treatment, although predicted fresh BaP concentrations at locations above 40°N were two or three times higher than the treatment without OA coating effects, the simulation still substantially underestimates the BaP concentrations in these regions by 50% (Fig. 6c). Moreover, model-estimated BaP concentrations in

https://doi.org/10.5194/egusphere-2024-3269
Preprint. Discussion started: 4 November 2024

ROI-T perform even worse at low latitudes compared to high latitudes. On a global average, the ROI-T approach, accounting for the temperature and humidity dependence of the phase state, diffusivity, and reactivity of particulate-bound BaP, underestimates BaP by ~60% in DJF (Fig. 5a, c).

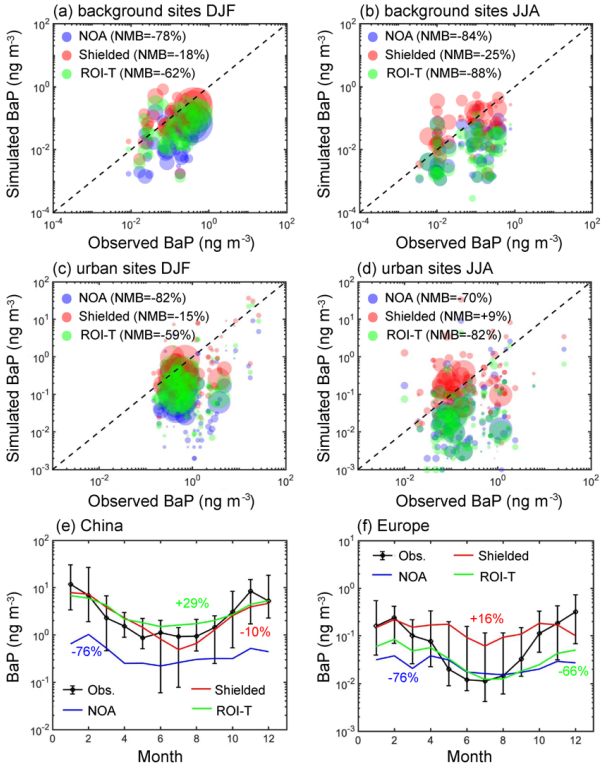

Figure 5. Comparison between simulated surface BaP concentrations from NOA, Shielded, and ROI-T simulations and ground-based measurements (a-b) for 66 background sites, (c-d) for 208 urban impacted sites. The circle area is proportional to the number of days sampled at each site. Annual variation of measured and simulated BaP concentrations at (e) 18 sites (6 background and 12 urban impacted sites) in China, and (f) 18 background sites in Europe. Black lines represent measured values (median and 15th and 85th percentiles of site monthly means), while blue (NOA), red (Shielded), and green (ROI-T) lines represent the median of the monthly model-simulated means for these sites.

In JJA, both NOA and ROI-T simulations struggle to capture BaP concentrations, underestimating observations by more than 70% (Fig. 5b and 5d). However, similar to DJF, the model-predicted concentrations in simulation using the Shielded approach exhibit the best agreement with ground measurements in JJA, showing a normalized mean bias of -25% and +9% at the background and urban-affected sites, respectively. Interestingly, the ROI-T approach deviates more from the actual observed values, especially at measurement locations between 40°N and 40°S (Fig. 6d and 6f).

https://doi.org/10.5194/egusphere-2024-3269
Preprint. Discussion started: 4 November 2024

Figure 5e indicates that both the Shielded simulation (red line) and ROI-T simulation (green line) capture the magnitude and seasonal variations of BaP concentrations compared with monthly observations at 18 sites in China (black lines). The simulated and observed BaP concentrations peak in winter but are lowest in summer. As mentioned in section 3.1, the predicted monthly variations in BaP concentrations are due to the seasonality of BaP emissions and BaP oxidation rates. For instance, residential emissions in China are four times higher in winter than in summer, contributing 78% of BaP emissions in winter and 56% in summer [Shen et al., 2013]. Furthermore, lower wintertime temperatures favor more viscous OA coatings to reduce BaP diffusion and decrease oxidation rates, while more liquid-like OA coatings in summer have a minor effect on BaP oxidation reactions. In contrast, although the models show a similar seasonal cycle to observations, fresh BaP concentrations are largely underestimated throughout the year in the absence of the OA coating effect (NOA).

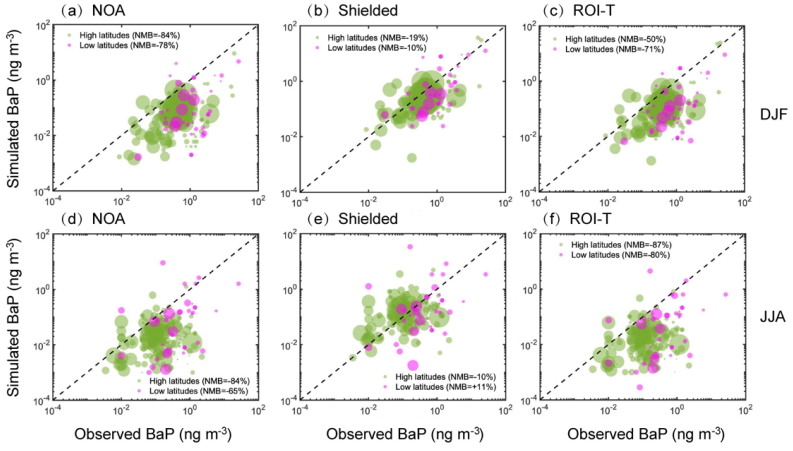

Figure 6. Comparison between simulated surface BaP concentrations at relatively high latitude regions (marked as olive, measured locations north of 40°N) and low latitude regions (marked as magenta, measured locations between 40°N and 40°S) in (a-c) DJF and (d-f) JJA, respectively. The circle area is proportional to the number of days sampled at each site. Both background and urban sites are included.

In Europe, although the simulated BaP for the Shielded approach also exhibits the best agreement with observations at 18 sites throughout the year, with a normalized mean bias of +16%, the simulated BaP fails to capture the magnitude of the measured BaP concentrations during the warm season (Fig. 5f). From April to October, model-predicted BaP concentrations in the Shielded simulation are overestimated by 88%. In contrast, the simulated BaP concentrations for the ROI-T approach are consistent with the monthly variation of the measured BaP concentrations, despite showing a 66% underestimated annual mean, which is mainly due to the significant underestimation in cool season. Our results suggest that while the Shielded simulation is likely closer to actual BaP magnitudes at mid- and low-latitudes, the ROI-T approach may better represent seasonal variation at mid-and high-latitudes but overestimates the coefficient of BaP multiphase degradation rates.

https://doi.org/10.5194/egusphere-2024-3269
Preprint. Discussion started: 4 November 2024

3.3.2 Oxidized BaP

Due to limited observations of oxidized BaP, specifically 1-, 3-, and 6-nitrobenzo(a)pyrene, we assess monthly changes in BaP for three different particle-bound BaP degradation approaches performed at two sites, Grenoble and SIRTA. In this study, we compare both simulated fresh BaP and oxidized BaP with in situ measurements. Note that the simulated fresh/oxidized BaP concentrations used for comparison in Grenoble are values after downscaling, as the site is centrally located and represents a location with significant urban influence. In contrast, the SIRTA site is located 25 km southwest of central Paris and is considered representative of regional background air quality. We, therefore, compare simulated fresh/oxidized BaP concentrations with coarse horizontal resolution to measurements at the SIRTA site.

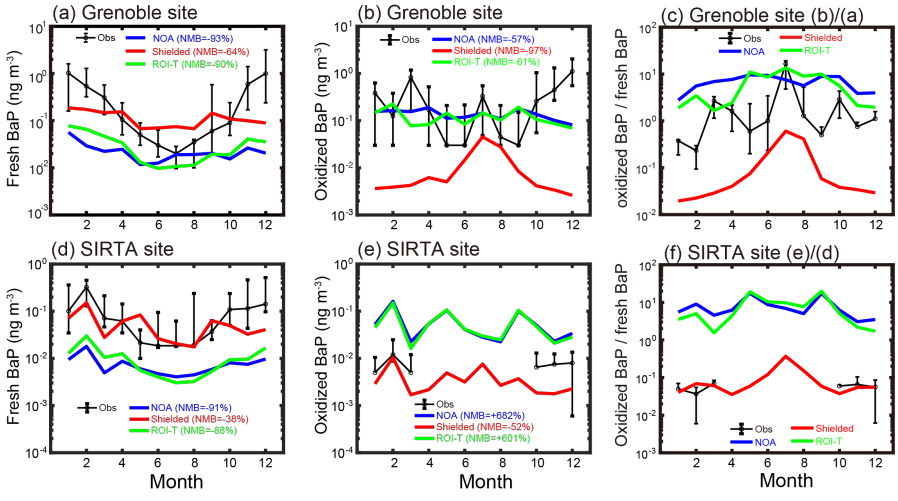

Figure 7. Monthly comparison between simulated surface fresh and oxidized BaP from NOA, Shielded, and ROI-T simulations and ground-based measurements at (a-c) Grenoble and (e-f) SIRTA sites. Black lines represent measured values (median and 15th and 85th percentiles of each site), while blue (NOA), red (Shielded), and green (ROI-T) lines represent the model-simulated median per month. The ratio of oxidized BaP to fresh BaP are represent in (c) and (f). From April to September at SIRTA site, observed concentrations of oxidized BaP were below LQ and therefore not presented on the graph.

The measurement site at the sampling station of "Les Frenes" in Grenoble (5.73ºE, 45.16ºN, France) represents the most densely populated urban area in Europe. Although the simulated concentrations applying the Shielded approach best match the observed fresh BaP concentrations in Grenoble among the three approaches, the model largely underestimates winter BaP concentrations but overestimates summer concentrations (Fig. 7a). Therefore, the assumption that viscous organic aerosol coatings completely shut off the reaction of fresh particle-bound BaP with ozone under cool and dry conditions is somewhat distorted and fails to capture seasonal variation in fresh BaP in Grenoble. The relatively low ratio of oxidized to fresh BaP using the Shielded approach in Fig. 7c indicates that the chemical scheme overly protects fresh PAHs from oxidation. Consequently, it underestimates oxidized BaP by one order

https://doi.org/10.5194/egusphere-2024-3269
Preprint. Discussion started: 4 November 2024

of magnitude. In contrast, despite the overall underestimation, the ROI-T simulation captures the seasonal variations in fresh BaP concentrations in Grenoble (Fig. 7a). However, the magnitude of the simulated oxidized BaP concentration is very similar to the observed values (Fig. 7b). As we mentioned above, the ratio of oxidized to fresh BaP in Fig. 7c reveals that the oxidation rate of BaP from fresh to oxidized is too fast under ROI-T treatment, especially during cold season.

In addition, the underestimation of both fresh and oxidized BaP concentrations may be partly due to the coarse horizontal resolution of simulated BaP, and inaccurate urban PAH emissions. We use a downscaling formulation to convert the 200 km grid resolution to a ~10 km grid resolution, but the spatial distribution of BaP obtained in this way is highly dependent on accurate emissions and meteorological fields. Previous studies have reported that traditional biomass combustion for residential heating is the main source of $PM_{2.5}$ in France in winter and including in the Grenoble area [Favez et al., 2009; 2021; Srivastava et al., 2018; Weber et al., 2019; Zhang et al., 2020a], thus inevitably emitting large amounts of BaP. Considering the underestimation of both fresh and oxidized BaP concentrations at the Grenoble site in winter, there is a large uncertainty in the emission and spatial distribution of PAHs in urban areas (Fig. 7a, b).

For the SIRTA site, the simulated BaP from the Shielded simulation shows good performance compared to the observed concentrations of fresh and oxidized BaP in winter (Fig. 7d, e). The performance of Shielded approach in summer remains unclear due to the lack of observed concentrations of oxidized BaP (Fig. 7e). However, the underestimation of fresh BaP concentrations and overestimation of oxidized BaP concentrations in ROI-T and NOA suggest that the particle-bound PAH degradation rate is too fast for these two approaches (Fig. 7c-d).

According to the ROI-T approach, once BaP is absorbed by organic aerosols, it can only be oxidized when it comes to the surface through bulk diffusion or O_3 absorption from the gas sorption layer to bulk layers. The changes in the BaP degradation rate coefficient are highly dependent on variations in temperature and relative humidity [Mu et al., 2018]. Considering that RH in the French winter is generally higher than 70% (Fig. 2b), the BaP degradation rate coefficient decreases by only one order of magnitude for every 20 K drop in temperature from around 293 K. Therefore, the oxidation rate of ROI-T for particle-bound PAHs is reduced by no more than 50% when the temperature is around 280 K in the French winter (Fig. 2a). Our results suggest that at higher humidity, the ROI-T approach underestimates the impact of OA coatings on PAH degradation effectiveness. Thus, the model's ability to simulate fresh BaP is not significantly enhanced over the default NOA when the ROI-T approach is elected, as relative humidity is significantly higher than 70% in mid- and high-latitude winters (Figs. 5f, 6c).

3.4. Lung-cancer risk of PAH mixture

As an indicator of cancer risk from PAH mixtures, previous studies calculated PAH-associated health risks based on exposure to BaP concentrations using a method grounded in epidemiological data [Bostrom et al., 2002; Zhang et al., 2009; Shen et al., 2014; Shrivastava et al., 2017; T Wang et al., 2017; Kelly et al., 2021]. These studies primarily considered fresh PAHs when assessing PAH-associated health risks. In this study, we follow the approach of previous studies to estimate ILCR [Shen et al., 2014; Shrivastava et al., 2017; Lou et al., 2023].

https://doi.org/10.5194/egusphere-2024-3269
Preprint. Discussion started: 4 November 2024

Figure 8a illustrates that global and regional population-weighted ILCR varies significantly across simulations when only considering exposure to fresh PAH. This variation is due to the substantial impact of PAH degradation approaches on fresh BaP concentrations. On a global population-weighted basis, the ILCR is predicted to be ~0.6×10^{-5} from the NOA and ROI-T simulations, falling within WHO-acceptable risk levels for PAH exposure. However, based on the Shielded simulation, the global population-weighted ILCR is predicted to be ~2×10^{-5}, exceeding the acceptable limit of 1 death per 100,000 persons. Moreover, without the heterogeneous oxidation of BaP, Shen et al. (2014) predicted an even higher global population-weighted ILCR of 3×10^{-5}. These results underscore the high sensitivity of global ILCR estimates to the choice of PAH degradation approaches.

The variations in fresh BaP exposure and population-weighted ILCR are even more important for regional estimation. Using the Shielded approach, the regional average population-weighted ILCR is predicted to exceed 1×10^{-5} over East Asia, South Asia, Southeast Asia, Russia, Africa, and South America. In contrast, ILCR for NOA and ROI-T simulations suggests a 3-4 times lower lung cancer risk in these regions, expected to be below 1×10^{-5} except in East Asia (Fig. 8a). Due to the high emission levels in 2008, the ROI-T simulation estimates a 50% higher ILCR than the NOA simulation, also exceeding the WHO acceptable limit in the East Asia.

Furthermore, recent laboratory studies suggest that oxidized PAHs persist in the particle-phase and often appear as higher molecular weight peaks in particle mass spectra [Ringuet et al., 2012; Zelenyuk et al., 2012; Keyte et al., 2013; Jariyasopit et al., 2014]. Some PAH oxidation products may even be more toxic than their parent compounds [EHC 2003; Clergé et al., 2019; Hrdina et al., 2022; Peng et al., 2023]. A quantitative understanding of the toxicity of these products is lacking, as each parent PAH could be oxidized into hundreds of products. In this study, we conduct a conservative first-order calculation of lung cancer risk associated with oxidized PAHs, assuming that PAH oxidation products have the same toxicity as their parents. On a global population-weighted basis, the ILCR is projected to 2.5 deaths per 100,000 persons when exposure to oxidized BaP is added to our previous calculations of fresh BaP exposure for all three simulation approaches (Fig. 8b). While three-quarters of the global population-weighted ILCR for the Shielded simulation is contributed to fresh PAH, oxidized PAHs contribute approximately 40% the ILCR in warm and humid regions such as South Asia, Southeast Asia, and Africa. In comparison, NOA and ROI-T simulations predict a dominant contribution of ILCR from PAH oxidation products compared to fresh PAHs over most regions of the globe. For example, over East Asia and South Asia, the NOA and ROI-T simulations predict that the regional population-weighted ILCR will exceed 3 deaths per 100,000 persons resulting from the oxidized PAHs alone, compared to ~1 death per 100,000 persons from oxidized PAHs in the Shielded simulation. The oxidized-fresh PAH ILCR split is much greater in the NOA and ROI-T simulations compared to the Shielded simulation.

Despite differences in organic coating effectiveness and heterogeneous reactivity between the NOA, Shielded, and ROI-T simulations, all schemes suggest that oxidized PAHs are crucial for lung cancer risk and cannot be neglected. If the toxicity of oxidized PAHs is similar to fresh PAHs, the total ILCR (fresh+oxidized) is comparable in the three approaches. However, oxidized PAHs could be much more important in certain regions (such as Southeast Asia, South Asia, and Africa), depending on their composition/toxicity and where the organic coatings are less effective in shielding them from heterogeneous reactivity. Considering the high levels of oxidized PAHs in mid-to-low latitudes, the

https://doi.org/10.5194/egusphere-2024-3269
Preprint. Discussion started: 4 November 2024

558 measurements for oxidized PAHs, as well as human health exposure to oxidized PAHs, are necessary
559 for further studies [Kelly et al., 2021].
560

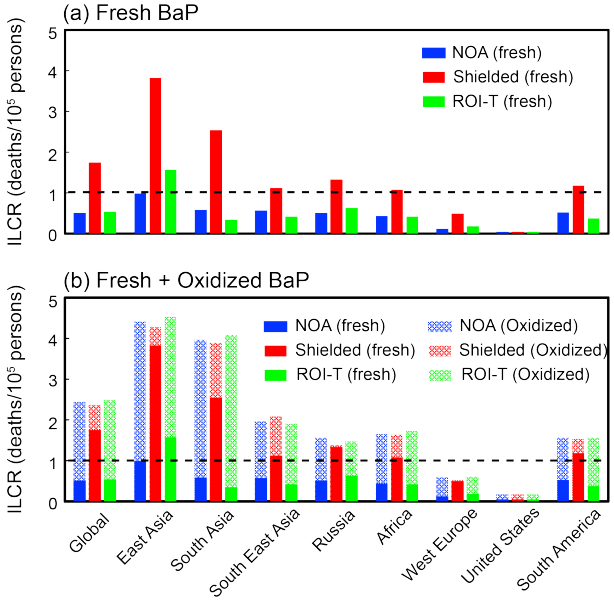

561

562 **Figure 8. Regional PAH-associated ILCR from NOA, Shielded, and ROI-T simulations. Note that solid bars**
563 **in (a, b) and shaded bars in (b) represent ILCR calculated from exposure to fresh and oxidized PAHs,**
564 **respectively.**

565 **4. Conclusion and Discussion**

566 This study uses the CAM5 model to investigate the impact of particle-bound PAH degradation
567 approaches on the spatial distribution of BaP, considering the presence or absence of OA coatings. The
568 three PAH degradation approaches are (1) OA coatings do not affect particle-bound BaP oxidation, (2)
569 the impact of OA coating on particle-bound BaP, assuming viscous OA coatings completely shield the
570 reaction of BaP with ozone under cool and dry conditions, and (3) the influence of OA coating on
571 particle-bound BaP degradation, assuming OA coatings slow down the oxidation reaction rate as a
572 function of temperature and humidity.
573 In general, the seasonal variation of BaP is highly dependent on changes in emissions, deposition, and
574 the chosen BaP degradation approach. In DJF, the demand for household activities such as cooking,
575 heating, and lighting increases, contributing to high BaP emissions. Additionally, less efficient wet
576 removal processes further enhance simulated BaP levels in DJF compared to JJA. The PWGA fresh BaP
577 concentration is predicted to be 0.24 ng m^{-3} without considering OA coatings, notably underestimating
578 measurements worldwide. In the absence of OA coatings, 82% of total BaP is rapidly oxidized near
579 source areas in DJF. The presence of viscous OA coatings slows down the oxidation process of fresh
580 BaP, resulting in a substantial increase in concentrations, ranging from 2 to 6 times in DJF. The Shielded

https://doi.org/10.5194/egusphere-2024-3269
Preprint. Discussion started: 4 November 2024

approach predicts the highest PWGA fresh BaP concentration of 1.30 ng m^{-3} in DJF. According to the Shieled simulation, most fresh BaP can persist in the atmosphere for several days, with only 10% of the total BaP being oxidized globally, mainly in the tropics. While the magnitudes and spatial distribution of fresh BaP concentrations are similar at high latitudes (e.g., Europe and North America) between the Shielded and the ROI-T approaches, the ROI-T approach, considering decreasing OA coating effectiveness with reduced temperature and RH, leads to lower fresh BaP concentrations in Africa, South Asia, and East Asia compared to the Shielded. Suprisingly, the ROI-T approach still predicts 71% of the total BaP to be oxidized globally in DJF.

In JJA, BaP concentrations are concentrated near the source areas. While the Shielded approach still predicts a much higher PWGA fresh BaP concentration than that without OA coating affect, the ROI-T approach predicts the lowest PWGA fresh BaP concentration of 0.04 ng m^{-3} due to even faster first-order reaction rate coefficients under warm and humidity concentrations. In comparison, all simulations predict that more than 90% of the total BaP is oxidized in JJA in the tropics (30°S-30°N). At mid-to-high latitudes, the oxidized BaP varies greatly with the OA coating assumpations. While 80-95% of the total BaP is oxidized in NOA or ROI-T simulations, the oxidized BaP contributes no more than 40% to the total BaP in the Shielded simulation.

In our model evaluation, we compare simulated fresh BaP concentrations with observations at 66 background/remote sites and 208 non-background sites globally. On a global basis, both NOA and ROI-T simulations perform poorly, underestimating fresh BaP concentrations by 60-80%. The Shielded approach predicts the best agreement with observations, with normalized mean bias always within ±20%. The choice of BaP degradation approach has significantly different effects on improving BaP simulations in various regions worldwide. For instance, both Shielded and ROI-T approaches improve the magnitude and seasonal variations of BaP concentrations in China. However, while the Shielded simulation is more aligned with the actual concentrations of BaP in Europe, our results indicate that the Shielded approach is somewhat distorted and fails to capture seasonal variation in fresh BaP.

Additionally, due to measurement limitations, concentrations of oxidized BaP from Grenoble in 2013 and from SIRTA in 2014-2015 are also used for model evaluation. Our results indicate that while the Shielded approach agrees best with the measured magnitude of BaP concentrations, this approach underestimates the oxidation rates, especially during the warm season. In contrast, although the ROI-T approach overstates the oxidation rates of BaP in multiphase environments, it offers a better depiction of seasonal variations in fresh BaP concentrations. Therefore, to improve global PAH simulations, further studies are needed to better understand the impact of OA coatings on PAH degradation effectiveness, either for the ROI-T approach at higher humidity or for the Shielded approach at room temperature. A broader range of observational data, including both ground-based and satellite-derived information (such as water-soluble organic aerosols [Zhang et al., 2020b]), could also be utilized to validate the model.

We also employ a methodology based on epidemiological data to estimate the PAH-associated ILCR. When calculated solely based on exposure to fresh BaP, the population-weighted ILCR varies largely among the three PAH degradation approach simulations. On a global population-weighted basis, the ILCR ranges from ~0.6×10^{-5} for the NOA and ROI-T simulations to ~2×10^{-5}, exceeding the acceptable limit of 1 death per 100,000 persons. Furthermore, when considering the toxicity of oxidized PAHs to be similar to their parent PAHs, the total ILCR (fresh+oxidized) remain comparable across the three approach simulations, amounting to 2.5 deaths per 100,000 persons. Oxidized PAHs may also be

https://doi.org/10.5194/egusphere-2024-3269
Preprint. Discussion started: 4 November 2024

important, depending on factors like their composition/toxicity and the effectiveness of OA coatings in shielding fresh PAHs from heterogeneous reactivity. This study underscores the significance of considering both fresh and oxidized PAHs in assessing cancer risk, particularly in regions where oxidized PAHs may play a substantial role.

Data availability

The ERA-Interim reanalysis data is available from https://www.ecmwf.int/en/forecasts/datasets/reanalysis-datasets/era-interim. The GEMS 0.1° × 0.1° global BaP emission inventory is available from gems.sustech.edu.cn. The long-term observation data are obtained from IADN (https://www.epa.gov/great-lakes-monitoring/great-lakes-integrated-atmospheric-deposition-network), EMEP (https://www.emep.int), and GENASIS (https://www.genasis.cz).

Competing interests

Manish Shrivastava is a member of the editorial board of ACP.

Acknowledgments

This research was supported by the National Natural Science Foundation of China (grant number: 42075095; 42293322), Fundamental Research Funds for the Central Universities (grant number: DLTD2107), the Laboratory Directed Research and Development programme at Pacific Northwest National Laboratory (PNNL), the Energy Exascale Earth System Model (E3SM) project, and the U.S. Department of Energy (DOE) Office of Science, Office of Biological and Environmental Research's Early Career Research programme. PNNL is operated for the DOE by Battelle Memorial Institute under Contract DE-AC05-76RL01830. ChatGPT was utilized to polish the English of this manuscript.

References

Ahad, J. M. E., Macdonald, R. W., Parrott, J. L., Yang, Z., Zhang, Y., Siddique, T., Kuznetsova, A., Rauert, C., Galarneau, E., Studabaker, W. B., Evans, M., McMaster, M. E., Shang, D.: Polycyclic aromatic compounds (PACs) in the Canadian environment: A review of sampling techniques, strategies and instrumentation, Environ. Pollut., 266(Pt 2), 114988, doi: https://doi.org/10.1016/j.envpol.2020.114988, 2020.

Arp, H. P., Schwarzenbach, R. P., and Goss, K. U.: Ambient gas/particle partitioning. 2: The influence of particle source and temperature on sorption to dry terrestrial aerosols, Environ. Sci. Technol., 42(16), 5951-5957, https://doi.org/10.1021/es703096p, 2008.

https://doi.org/10.5194/egusphere-2024-3269
Preprint. Discussion started: 4 November 2024

Berkemeier, T., Steimer, S. S., Krieger, U. K., Peter, T., Poschl, U., Ammann, M., and Shiraiwa, M.: Ozone uptake on glassy, semi-solid and liquid organic matter and the role of reactive oxygen intermediates in atmospheric aerosol chemistry, Phys. Chem. Chem. Phys., 18(18), 12662-12674, https://doi.org/10.1039/C6CP00634E, 2016.

Bateman, A. P., Bertram, A. K., and Martin, S. T.: Hygroscopic influence on the semisolid-to-liquid transition of secondary organic materials, J. Phys. Chem. A, 119(19), 4386-4395, dx.doi.org/10.1021/jp508521c, 2015.

Boffetta, P., Jourenkova, N., and Gustavsson, P.: Cancer risk from occupational and environmental exposure to polycyclic aromatic hydrocarbons, Cancer Causes & Control, 8(3), 444-472, doi:10.1023/a:1018465507029, 1997.

Boruvkova, J.: GENASIS-Global Environmental Assessment and Information System, version 2.0., Masaryk University, www.genasis.cz, 2015.

Bostrom, C. E., Gerde, P. , Hanberg, A., Jernstrom, B., Johansson, C., Kyrklund, T., Rannug, A., Tornqvist, M., Victorin, K., and Westerholm, R.: Cancer risk assessment, indicators, and guidelines for polycyclic aromatic hydrocarbons in the ambient air, Environ. Health Perspect., 110, 451-488, doi:10.1289/ehp.110-1241197, 2002.

Brown, A. S., Brown, R. J., Coleman, P. J., Conolly, C., Sweetman, A. J., Jones, K. C., Butterfield, D. M., Sarantaridis, D., Donovan, B. J., and Roberts, I.: Twenty years of measurement of polycyclic aromatic hydrocarbons (PAHs) in UK ambient air by nationwide air quality networks, Environ Sci: Process. Impacts., 15(6), doi:10.1039/c3em00126a, 1199-1215, 2013.

Cazaunau, M., Ménach, K. Le, Budzinski, H., and Villenave, E.: Atmospheric heterogeneous reactions of Benzo(a)pyrene, Z. für Phys. Chem., 224, 1151-1170, https://doi.org/10.1524/zpch.2010.6145, 2010.

Chen, S.-C., and Liao, C.-M.: Health risk assessment on human exposed to environmental polycyclic aromatic hydrocarbons pollution sources, Sci. Total Environ., 366(1), 112-123, https//doi.org/10.1016/j.scitotenv.2005.08.047, 2006.

Clergé, A., Le Goff, J., Lopez, C., Ledauphin, J., and Delépée, R.: Oxy-PAHs: occurrence in the environment and potential genotoxic/mutagenic risk assessment for human health, Critical reviews in toxicology, 49(4), 302-328, doi:10.1080/10408444.2019.1605333, 2019.

CPCB (Central Pollution Control Board): National Ambient Air Quality Monitoring Programme (NAAQMS) Report No. 45/2019-2020, Ministry of Environment, Forest and Climate Change, Government of India, New Delhi, India, 2020.

Crippa, M., Guizzardi, D., Muntean, M., Schaaf, E., Dentener, F., van Aardenne, J. A., Monni, S., Doering, U., Olivier, J. G. J., Pagliari, V., and Janssens-Maenhout, G: Gridded emissions of air pollutants for the period 1970-2012 within EDGAR v4.3.2, Earth Syst. Sci. Data, 10(4), 1987-2013, https://doi.org/10.5194/essd-10-1987-2018, 2018.

Delgado-Saborit, Stark, J. M., C., and Harrison, R. M.: Carcinogenic potential, levels and sources of polycyclic aromatic hydrocarbon mixtures in indoor and outdoor environments and their implications for air quality standards, Environ. Int., 37(2), 383-392, doi:10.1016/j.envint.2010.10.011, 2011.

Emmons, L. K., Walters, S., Hess, P. G., Lamarque, J.-F., Pfister, G. G., Fillmore, D., Granier, C., Guenther, A., Kinnison, D., Laepple, T., Orlando, J., Tie, X., Tyndall, G., Wiedinmyer, C., Baughcum, S. L., and Kloster, S.: Description and evaluation of the Model for Ozone and Related chemical Tracers,

https://doi.org/10.5194/egusphere-2024-3269
Preprint. Discussion started: 4 November 2024

version 4 (MOZART-4), Geosci. Model Dev., 3(1), 43-67, https://doi.org/10.5194/gmd-3-43-2010, 2010.

HEC (Environmental Health Criteria) 229: Selected nitro- and nitro-oxy-polycyclic aromatic hydrocarbons, WHO Library, https://www.inchem.org/documents/ehc/ehc/ehc229.htm, 2003.

EPA (Environmental Protection Agency): Air Quality Criteria for Particulate Matter (EPA/600/P-99/002aF, EPA/600/P-99/002bF), Office of Research and Development, Washington, DC, USA, 2004.

EPCEU (European Parliament and Council of the European Union): Directive 2004/107/EC of the European Parliament and of the Council of 15 December 2004 relating to arsenic, cadmium, mercury, nickel and polycyclic aromatic hydrocarbons in ambient air, Official Journal of the European Union, L23, 3-16, 2004.

Esteve, W., Budzinski, H., and Villenave, E.: Relative rate constants for the heterogeneous reactions of NO and OH radicals with polycyclic aromatic hydrocarbons adsorbed on carbonaceous particles. Part 2: PAHs adsorbed on diesel particulate exhaust SRM 1650a, Atmos. Environ., 40(2), 201-211, https://doi.org/10.1016/j.atmosenv.2005.07.053, 2006.

Famiyeh, L., Chen, K., Xu, J., Sun, Y., Guo, Q., Wang, C., Lv, J., Tang, Y.-T., Yu, H., Snape, C., He, J.: A review on analysis methods, source identification, and cancer risk evaluation of atmospheric polycyclic aromatic hydrocarbons, Sci. Total. Environ., 789, 147741, 2021.

Favez, O., Cachier, H., Sciare, J., Sarda-Estève, R., and Martinon L.: Evidence for a significant contribution of wood burning aerosols to PM during the winter season in Paris, France, Atmos. Environ., 43(22-23), 3640-3644, https://doi.org/10.1016/j.atmosenv.2009.04.035, 2009.

Favez, O., Weber, S., Petit, J.-E., Alleman, L. Y., Albinet, A., Riffault, V., Chazeau, B., Amodeo, T., Salameh, D., Zhang, Y., Srivastava, D., Samaké, A., Aujay-Plouzeau, R., Papin, A., Bonnaire, N., Boullanger, C., Chatain, M., Chevrier, F., Detournay, A., Dominik-Sègue, M., Falhun, R., Garbin, C., Ghersi, V., Grignion, G., Levigoureux, G., Pontet, S., Rangognio, J., Zhang, S., Besombes, J.-L., Conil, S., Uzu, G., Savarino, J., Marchand, N., Gros, V., Marchand, C., Jaffrezo, J.-L., and Leoz-Garziandia, E.: Overview of the French Operational Network for In Situ Observation of PM Chemical Composition and Sources in Urban Environments (CARA Program), Atmosphere, 12, 207, https://doi.org/10.3390/atmos12020207, 2021.

Friedman, C. L., Pierce, J. R., and Selin, N. E.: Assessing the influence of secondary organic versus primary carbonaceous aerosols on long-range atmospheric polycyclic aromatic hydrocarbon transport, Environ Sci Technol, 48(6), 3293-3302, https://doi.org/10.1021/es405219r, 2014.

Galarneau, E., Makar, P. A., Zheng, Q., Narayan, J., Zhang, J., Moran, M. D., Bari, M. A., Pathela, S., Chen, A. and Chlumsky, R.: PAH concentrations simulated with the AURAMS-PAH chemical transport model over Canada and the USA, Atmos. Chem. Phys., 14(8), 4065-4077, https://doi.org/10.5194/acp-14-4065-2014, 2014.

Halsall, C. J., Barrie, L. A., Fellin, P., Muir, D. C. G., Billeck, B. N., Lockhart, L., Rovinsky, F. Y., . Kononov, E. Y., and Pastukhov, B.: Spatial and temporal variation of polycyclic aromatic hydrocarbons in the Arctic atmosphere, Environ. Sci. Technol., 31(12), 3593-3599, https://doi.org/10.1021/es970342d, 1997.

Han, F., Guo, H., Hu, J., Zhang, J., Ying, Q., and Zhang, H.: Sources and health risks of ambient polycyclic aromatic hydrocarbons in China, Sci Total Environ, 698, 134229, https://doi.org/10.1016/j.scitotenv.2019.134229, 2020.

https://doi.org/10.5194/egusphere-2024-3269
Preprint. Discussion started: 4 November 2024

Han, F., Kota, S. H., Sharma, S., Zhang, J., Ying, Q., and Zhang, H.: Modeling polycyclic aromatic hydrocarbons in India: Seasonal variations, sources and associated health risks, Environ Res, 212(Pt D), 113466, https://doi.org/10.1016/j.envres.2022.113466, 2022.

Han, J., Liang, Y. S., Zhao, B., Wang, Y., Xing, F. T., and Qin, L. B.: Polycyclic aromatic hydrocarbon (PAHs) geographical distribution in China and their source, risk assessment analysis, Environ. Pollut., 251, 312-327, https://doi.org/10.1016/j.envpol.2019.05.022, 2019.

Hrdina, A. I. H., Kohale, I. N., Kaushal, S., Kelly, J., Selin, N. E., Engelward, B. P., and Kroll, J. H.: The parallel transformations of polycyclic aromatic hydrocarbons in the body and in the atmosphere, Environ. Health Perspect., 130(2), 025004, https://doi.org/10.1289/EHP9984, 2022.

Hu, R., Liu, G., Zhang, H., Xue, H., and Wang, X.: Levels and Sources of PAHs in Air-borne PM(2.5) of Hefei City, China, Bull. Environ. Contam. Toxicol., 98(2), 270-276, doi:10.1007/s00128-016-2019-9, 2017.

Hu, R., Liu, G., Zhang, H., Xue, H., Wang, X., and Wang, R.: Particle-Associated Polycyclic Aromatic Hydrocarbons (PAHs) in the Atmosphere of Hefei, China: Levels, Characterizations and Health Risks, Arch. Environ. Contam. Toxicol., 74(3), 442-451, doi:10.1007/s00244-017-0472-z, 2018.

Hung, H., Kallenborn, R., Breivik, Knut, Su, Y., Brorström-Lundén, E., Olafsdottir, K., Thorlacius, J. M., Leppänen, S., Bossi, R., Skov, H., Manø, S., Patton, G. W., Stern, G., Sverko, E., and Fellin, P.: Atmospheric monitoring of organic pollutants in the Arctic under the Arctic Monitoring and Assessment Programme (AMAP): 1993-2006, Sci Total Environ, 408(15), 2854-2873, doi:10.1016/j.scitotenv.2009.10.004, 2010.

IARC: Some non-heterocyclic polycyclic aromatic hydrocarbons and some related exposures, IARC Monographs on the Evaluation of Carcinogenc Risks to Humans, 92, 1-853, ISBN-13, 978-92-832-1292-8, 978-92-832-1292-9, 2010.

IARC: International Agency for Research on Cancer (IARC) monographs on the identification of carcinogenic hazards to humans, Agents Classified by the IARC Monographs, https://monographs.iarc.who.int/list-of-classifications, 2021.

Iakovides, M., Apostolaki, M., and Stephanou, E. G.: PAHs, PCBs and organochlorine pesticides in the atmosphere of Eastern Mediterranean: Investigation of their occurrence, sources and gas-particle partitioning in relation to air mass transport pathways, Atmos. Environ., 244, 117931, https://doi.org/10.1016/j.atmosenv.2020.117931, 2021.

Janssens-Maenhout, G., Crippa, M., Guizzardi, D., Dentener, F., Muntean, M., Pouliot, G., Keating, T., Zhang, Q., Kurokawa, J., Wankmüller, R., van der Gon, H. D., Kuenen, J. J. P., Klimont, Z., Frost, G., Darras, S., Koffi, B., and Li, M.: HTAP_v2.2: a mosaic of regional and global emission grid maps for 2008 and 2010 to study hemispheric transport of air pollution, Atmos. Chem. Phys., 15(19), 11411-11432, https://doi.org/10.5194/acp-15-11411-2015, 2015.

Jariyasopit, N., McIntosh, M., Zimmermann, K., Arey, J., Atkinson, R., Cheong, P. H., Carter, R. G., Yu, T. W., Dashwood, R. H., and Massey Simonich, S. L.: Novel nitro-PAH formation from heterogeneous reactions of PAHs with NO2, NO3/N2O5, and OH radicals: prediction, laboratory studies, and mutagenicity, Environ. Sci. Technol., 48(1), 412-419, https://doi.org/10.1021/es4043808, 2014.

Kahan, T. F., Kwamena, N. O. A., and Donaldson D. J.: Heterogeneous ozonation kinetics of polycyclic aromatic hydrocarbons on organic films, Atmos. Environ., 40(19), 3448-3459, https://doi.org/10.1016/j.atmosenv.2006.02.004, 2006.

https://doi.org/10.5194/egusphere-2024-3269
Preprint. Discussion started: 4 November 2024

Keith, L. H.: The source of US EPA's sixteen PAH priority pollutants, Polycyclic Aromatic Compounds, 35(2-4), 147-160, https://doi.org/10.1080/10406638.2014.892886, 2015.

Kelly, J. M., Ivatt, P. D., Evans, M. J., Kroll, J. H., Hrdina, A. I. H., Kohale, I. N., White, F. M., Engelward, B. P., and Selin, N. E.: Global Cancer Risk From Unregulated Polycyclic Aromatic Hydrocarbons, Geohealth, 5(9), e2021GH000401, https://doi.org/10.1029/2021GH000401, 2021.

Keyte, I. J., Harrison, R. M., and Lammel, G.: Chemical reactivity and long-range transport potential of polycyclic aromatic hydrocarbons--a review, Chem. Soc. Rev., 42(24), 9333-9391, https://doi.org/10.1039/C3CS60147A, 2013.

Kim, J. Y., Lee, J. Y., Choi, S. D., Kim, Y. P., and Ghim, Y. S.: Gaseous and particulate polycyclic aromatic hydrocarbons at the Gosan background site in East Asia, Atmos. Environ., 49, 311-319, https://doi.org/10.1016/j.atmosenv.2011.11.029, 2012.

Kim, K.-H., Jahan, S. A., Kabir, E., and Brown, R. J. C.: A review of airborne polycyclic aromatic hydrocarbons (PAHs) and their human health effects, Environment International, 60, 71-80, https://doi.org/10.1016/j.envint.2013.07.019, 2013.

Koop, T., Bookhold, J., Shiraiwa, M., and Poschl, U.: Glass transition and phase state of organic compounds: dependency on molecular properties and implications for secondary organic aerosols in the atmosphere, Phys. Chem. Chem. Phys., 13(43), 19238-19255, doi:10.1039/c1cp22617g, 2011.

Kumar, A., Sankar, T. K., Sethi, S. S., and Ambade, B.: Characteristics, toxicity, source identification and seasonal variation of atmospheric polycyclic aromatic hydrocarbons over East India, Environ. Sci. Pollut. Res. Int., 27(1), 678-690, doi:10.1007/s11356-019-06882-5, 2020.

Kwamena, N. O. A., Thornton, J. A., and Abbatt, J. P. D.: Kinetics of surface-bound benzo[a]pyrene and ozone on solid organic and salt aerosols, J. Phys. Chem. A, 108(52), 11626-11634, https://doi.org/10.1021/jp046161x, 2004.

Lammel, G., Dvorská, A., Klánová, J., Kohoutek, J., Kukacka, P., Prokes, R., and Sehili, A. M.: Long-range Atmospheric Transport of Polycyclic Aromatic Hydrocarbons is Worldwide Problem - Results from Measurements at Remote Sites and Modelling, Acta. Chim. Slov., 62(3), 729-735, doi:10.17344/acsi.2015.1387, 2015.

Lanzafame, G. M., Srivastava, D., Favez, O., Bandowe, B. A. M., Shahpoury, P., Lammel, G., Bonnaire, N., Alleman, L. Y., Couvidat, F., Bessagnet, B., Albinet, A.: One-year measurements of secondary organic aerosol (SOA) markers in the Paris region (France): Concentrations, gas/particle partitioning and SOA source apportionment, Sci. Total Environ., 757, 143921, https://doi.org/10.1016/j.scitotenv.2020.143921, 2021.

Lee, J. Y., Kim, Y. P., and Kang, C. H.: Characteristics of the ambient particulate PAHs at Seoul, a mega city of Northeast Asia in comparison with the characteristics of a background site, Atmos. Res., 99(1), https://doi.org/10.1016/j.atmosres.2010.09.029, 50-56, 2011.

Lhotka, R., Pokorná, P., and Zíková, N.: Long-Term Trends in PAH Concentrations and Sources at Rural Background Site in Central Europe, Atmosphere, 10(11), 687, https://doi.org/10.3390/atmos10110687, 2019.

Li, Y., Zhu, Y., Liu, W., Yu, S., Tao, S., and Liu, W.: Modeling multimedia fate and health risk assessment of polycyclic aromatic hydrocarbons (PAHs) in the coastal regions of the Bohai and Yellow Seas, Sci. Total Environ., 818, 151789, https://doi.org/10.1016/j.scitotenv.2021.151789, 2022.

https://doi.org/10.5194/egusphere-2024-3269
Preprint. Discussion started: 4 November 2024

Liu, X., Easter, R. C., Ghan, S. J., Zaveri, R., Rasch, P., Shi, X., Lamarque, J.-F., Gettelman, A., Morrison, H., Vitt, F., Conley, A., Park, S., Neale, R., Hannay, C., Ekman, A. M. L., Hess, P., Mahowald, N., Collins, W., Iacono, M. J., Bretherton, C. S., Flanner, M. G., and Mitchell, D.: Toward a minimal representation of aerosols in climate models: description and evaluation in the Community Atmosphere Model CAM5, Geosci. Model Dev., 5(3), 709-739, https://doi.org/10.5194/gmd-5-709-2012, 2012.

Liu, Y., Yan, C., Ding, X., Wang, X., Fu, Q., Zhao, Q., Zhang, Y., Duan, Y., Qiu, X., and Zheng, M.: Sources and spatial distribution of particulate polycyclic aromatic hydrocarbons in Shanghai, China, Sci. Total Environ., 584, 307-317, https://doi.org/10.1016/j.scitotenv.2016.12.134, 2017.

Lohmann, R., and Lammel, G.: Adsorptive and absorptive contributions to the gas-particle partitioning of polycyclic aromatic hydrocarbons: state of knowledge and recommended parametrization for modeling, Environ. Sci. Technol., 38(14), 3793-3803, https://doi.org/10.1021/es035337q, 2004.

Lou, S., Shrivastava, M., Ding, A., Easter, R. C., Fast, J. D., Rasch, P. J., Shen, H., Massey Simonich, S. L., Smith, S. J., and Tao, S.: Shift in Peaks of PAH‐Associated Health Risks From East Asia to South Asia and Africa in the Future, Earth's Future, 11(6), e2022EF003185, https://doi.org/10.1029/2022EF003185, 2023.

Ma, W.-L., Liu, L.-Y., Jia, H.-L., Yang, M., and Li, Y.-F.: PAHs in Chinese atmosphere Part I: Concentration, source and temperature dependence, Atmospheric Environment, 173, 330-337, https://doi.org/10.1016/j.atmosenv.2017.11.029, 2018.

Masclet, P., Hoyau, V., Jaffrezo, J. L., and Cachier H.: Polycyclic aromatic hydrocarbon deposition on the ice sheet of Greenland. Part I: superficial snow, Atmos. Environ., 34, 3195-3207, https://doi.org/10.1016/S1352-2310(99)00196-X, 2000.

Matthias, V., Aulinger, A. and Quante, M.: CMAQ simulations of the benzo(a)pyrene distribution over Europe for 2000 and 2001, Atmos. Environ., 43(26), 4078-4086, https://doi.org/10.1016/j.atmosenv.2009.04.058, 2009.

MEPPRC (Ministry of Environmental Protection of the People's Republic of China): Water quality - Derermination of polycyclic aromatic hydrocarbons - Liquid-liquid extraction and solid-phase extraction followed by high performance liquid chromatographic method, Nathional Environmental Protection Standards HJ 478-2009, Beijing, China, pp1-10, in Chinese, 2009.

Mu, Q., Shiraiwa, M., Octaviani, M., Ma, N., Ding, A., Su, H., Lammel, G., Poschl, U., and Cheng, Y.: Temperature effect on phase state and reactivity controls atmospheric multiphase chemistry and transport of PAHs, Sci. Adv., 4(3), doi:10.1126/sciadv.aap7314, 2018.

Muir, D., Bossi, R., Carlsson, P., Evans, M., De Silva, A., Halsall, C., Rauert, C., Herzke, D., Hung, H., Letcher, R., Rigét, F., and Roos, A.: Levels and trends of poly- and perfluoroalkyl substances in the Arctic environment - An update, Emerg. Contam., 5, 240-271, https://doi.org/10.1016/j.emcon.2019.06.002, 2019.

Munyeza, C. F., Rohwer, E. R., and Forbes, P. B. C.: A review of monitoring of airborne polycyclic aromatic hydrocarbons: An African perspective, Trends Anal. Chem., 24, e00070, https://doi.org/10.1016/j.teac.2019.e00070, 2019.

Niu J., Sun, P., and Schramm, K.-W.: Photolysis of polycyclic aromatic hydrocarbons associated with fly ash particles under simulated sunlight irradiation, Journal of Photochemistry and Photobiology A: Chemistry, 186(1), 93-98, https://doi.org/10.1016/j.jphotochem.2006.07.016, 2007.

https://doi.org/10.5194/egusphere-2024-3269
Preprint. Discussion started: 4 November 2024

Peng, B., Dong, Q., Li, F., Wang, T., Qiu, X., and Zhu, T.: A systematic review of polycyclic aromatic hydrocarbon derivatives: occurrences, levels, biotransformation, exposure biomarkers, and toxicity, Environmental Science & Technology, 57(41), 15314-15335, https://doi.org/10.1021/acs.est.3c03170, 2023.

Perera, F. P. J. S.: Environment and cancer: who are susceptible?, Science, 278(5340), 1068-1073, doi:10.1126/science.278.5340.1068, 1997.

Pöschl, U., Letzel, T., Schauer, C., and Niessner, R.: Interaction of ozone and water vapor with spark discharge soot aerosol particles coated with benzo [a] pyrene: O3 and H2O adsorption, benzo [a] pyrene degradation, and atmospheric implications, J. Phys. Chem. A, 105(16), 4029-4041, https://doi.org/10.1021/jp004137n, 2001.

Radonić, J., Jovčić Gavanski, N., Ilić, M., Popov, S., Očovaj, S. B., Vojinović Miloradov, M., and Turk Sekulić, M.: Emission sources and health risk assessment of polycyclic aromatic hydrocarbons in ambient air during heating and non-heating periods in the city of Novi Sad, Serbia, Stoch. Environ. Res. Risk Assess., 31(9), 2201-2213, doi:10.1007/s00477-016-1372-x, 2017.

Ringuet, J., Albinet, A., Leoz-Garziandia, E., Budzinski, H., and Villenave, E.: Reactivity of polycyclic aromatic compounds (PAHs, NPAHs and OPAHs) adsorbed on natural aerosol particles exposed to atmospheric oxidants, Atmos. Environ., 61, 15-22, https://doi.org/10.1016/j.atmosenv.2012.07.025, 2012.

Saukko, E., Lambe, A. T., Massoli, P., Koop, T., Wright, J. P., Croasdale, D. R., Pedernera, D. A., Onasch, T. B., Laaksonen, A., Davidovits, P., Worsnop, D. R., and Virtanen, A.: Humidity-dependent phase state of SOA particles from biogenic and anthropogenic precursors, Atmos. Chem. Phys., 12, 7517-7529, doi:10.5194/acp-12-7517-2012, 2012.

Schauer, C., Niessner, R., and Poschl, U.: Polycyclic aromatic hydrocarbons in urban air particulate matter: decadal and seasonal trends, chemical degradation, and sampling artifacts, Environ. Sci. Technol., 37(13), 2861-2868, https://doi.org/10.1021/es034059s, 2003.

Sehili, A. M., and Lammel, G.: Global fate and distribution of polycyclic aromatic hydrocarbons emitted from Europe and Russia, Atmos. Environ., 41(37), 8301-8315, https://doi.org/10.1016/j.atmosenv.2007.06.050, 2007.

Shahpoury, P., Lammel, G., Albinet, A., Sofuoglu, A., Dumanoglu, Y., Sofuoglu, S. C., Wagner, Z., and Zdimal, V.: Evaluation of a Conceptual Model for Gas-Particle Partitioning of Polycyclic Aromatic Hydrocarbons Using Polyparameter Linear Free Energy Relationships, Environ. Sci. Technol., 50(22), 12312-12319, https://doi.org/10.1021/acs.est.6b02158, 2016.

Shen, H., Tao, S., Liu, J., Huang, Y., Chen, H., Li, W., Zhang, Y., Chen, Y., Su, S., Lin, N., Xu, Y., Li, B., Wang, X., and Liu, W.: Global lung cancer risk from PAH exposure highly depends on emission sources and individual susceptibility, Sci. Rep., 4, 6561, https://doi.org/10.1038/srep06561, 2014.

Shen, H., Huang, Y., Wang, R., Zhu, D., Li, W., Shen, G., Wang, B., Zhang, Y., Chen, Y., Lu, Y., Chen, H., Li, T., Sun, K., Li, B., Liu, W., Liu, J., and Tao, S.: Global Atmospheric Emissions of Polycyclic Aromatic Hydrocarbons from 1960 to 2008 and Future Predictions, Environ. Sci. Technol., 47(12), 6415-6424, doi:10.1021/es400857z, 2013.

Srivastava, D., Tomaz, S., Favez, O., Lanzafame, G. M., Golly, B., Besombes, J.-L., Alleman, L. Y., Jaffrezo, J.-L., Jacob, V., Perraudin, E., Villenave, E. and Albinet, A.: Speciation of organic fraction

https://doi.org/10.5194/egusphere-2024-3269
Preprint. Discussion started: 4 November 2024

does matter for source apportionment. Part 1: A one-year campaign in Grenoble (France), Sci. Total Environ., 624, 1598–1611, https://doi.org/10.1016/j.scitotenv.2017.12.135, 2018.

Shiraiwa, M., Ammann, M., Koop, T., and Pöschl, U.: Gas uptake and chemical aging of s emisolid organic aerosol particles, Proc. Natl. Acad. Sci. U.S.A., 108(27), 11003-11008, https://doi.org/10.1073/pnas.1103045108, 2011.

Shiraiwa, M., Li, Y., Tsimpidi, A. P., Karydis, V. A., Berkemeier, T., Pandis, S. N., Lelieveld, J., Koop, T., and Pöschl, U.: Global distribution of particle phase state in atmospheric secondary organic aerosols, Nat Commun, 8(1), 15002, https://doi.org/10.1038/ncomms15002, 2017.

Shrivastava, M., Easter, R. C., Liu, X., Zelenyuk, A., Singh, B., Zhang, K., Ma, P.-L., Chand, D., Ghan, S., Jimenez, J. L., Zhang, Q., Fast, J., Rasch, P. J., and Tiitta, P.: Global transformation and fate of SOA: Implications of low-volatility SOA and gas-phase fragmentation reactions, J. Geophys. Res.: Atmos., 120(9), 4169-4195, https://doi.org/10.1002/2014JD022563, 2015.

Shrivastava, M., Lou, S., Zelenyuk, A., Easter, R. C., Corley, R. A., Thrall, B. D., Rasch, P. J., Fast, J. D., Massey Simonich, S. L., Shen, H., and Tao, S.: Global long-range transport and lung cancer risk from polycyclic aromatic hydrocarbons shielded by coatings of organic aerosol, Proc. Natl. Acad. Sci. U.S.A., 114(6), 1246-1251, https://doi.org/10.1073/pnas.1618475114, 2017.

Tomaz, S., P. Shahpoury, J. L. Jaffrezo, G. Lammel, E. Perraudin, E. Villenave, and A. Albinet (2016), One-year study of polycyclic aromatic compounds at an urban site in Grenoble (France): Seasonal variations, gas/particle partitioning and cancer risk estimation, Sci Total Environ, 565, 1071-1083.

Tørseth, K., Aas, W., Breivik, K., Fjæraa, A. M., Fiebig, M., Hjellbrekke, A.-G., Lund Myhre, C., Solberg, S., and Yttri, K. E.: Introduction to the European Monitoring and Evaluation Programme (EMEP) and observed atmospheric composition change during 1972–2009, Atmos. Chem.

Phys., 12(12), 5447-5481, doi:10.5194/acp-12-5447-2012, 2012.

van der Werf, G. R., Randerson, J. T., Giglio, L., Collatz, G. J., Mu, M., Kasibhatla, P. S., Morton, D. C., DeFries, R. S., Jin, Y., and van Leeuwen, T. T.: Global fire emissions and the contribution of deforestation, savanna, forest, agricultural, and peat fires (1997-2009), Atmos. Chem. Phys., 10(23), 11707-11735, https://doi.org/10.5194/acp-10-11707-2010, 2010.

Van Overmeiren, P., Demeestere, K., Wispelaere, P. D., Gili, S., Mangold, A., Causmaecker, K. D., Mattielli, N., Delcloo, A., Langenhove, H. V., and Walgraeve, C.: Four years of active sampling and measurement of atmospheric polycyclic aromatic hydrocarbons and oxygenated polycyclic aromatic hydrocarbons in Dronning Maud Land, East Antarctica, Environ. Sci. Technol., 58, 1577-1588, https://doi.org/10.1021.acs.est.3c06425, 2024.

Wang, T., Xia, Z. H., Wu, M. M., Zhang, Q. Q., Sun, S. Q., Yin, J., Zhou, Y. C., and Yang, H.: Pollution characteristics, sources and lung cancer risk of atmospheric polycyclic aromatic hydrocarbons in a new urban district of Nanjing, China, J. Environ. Sci., 55, 118-128, https://doi.org/10.1016/j.jes.2016.06.025, 2017.

Wang, W., Simonich, S., Giri, B., Chang, Y., Chang, Y., Zhang, Y., Jia. Y., Tao, S., Wang, R., Wang, B., Li, W., Cao, J., and Lu, X.: Atmospheric concentrations and air-soil gas exchange of polycyclic aromatic hydrocarbons (PAHs) in remote, rural village and urban areas of Beijing-Tianjin region, North China, Sci. Total. Environ., 409(15), 2942-2950, https://doi.org/10.1016/j.scitotenv.2011.04.021, 2011.

Weber, S., Salameh, D., Albinet, A., Alleman, L. Y., Waked, A., Besombes, J.-L., Jacob, V., Guillaud, G., Meshbah, B., Rocq, B., Hulin, A., Dominik-Sègue, M., Chrétien, E., Jaffrezo, J.-L., and Favez, O.:

https://doi.org/10.5194/egusphere-2024-3269
Preprint. Discussion started: 4 November 2024

Comparison of PM10 Sources Profiles at 15 French Sites Using a Harmonized Constrained Positive Matrix Factorization Approach, Atmos., 10, 310, https://doi.org/10.3390/atmos10060310, 2019.

WHO: Air quality guidelines for Europe, World Health Organization. Regional Office for Europe, 2000.

Zelenyuk, A., Imre, D., Beranek, J., Abramson, E., Wilson, J., and Shrivastava, M.: Synergy between secondary organic aerosols and long-range transport of polycyclic aromatic hydrocarbons, Environ. Sci. Technol., 46(22), 12459-12466, https://doi.org/10.1021/es302743z, 2012.

Zhang, Y., Albinet, A., Petit, J.-E., Jacob, V., Chevrier, F., Gille, G., Pontet, S., Chrétien, E., Dominik-Sègue, M., Levigoureux, G., Močnik, G., Gros, V., Jaffrezo, J.-L., and Favez, O.: Substantial brown carbon emissions from wintertime residential wood burning over France, Sci. Total Environ., 743, 140752, https://doi.org/10.1016/j.scitotenv.2020.140752, 2020a.

Zhang, Y., Li, Z., Chen, Y., de Leeuw, G., Zhang, C., Xie, Y., and Li, K.: Improved inversion of aerosol components in the atmospheric column from remote sensing data, Atmos. Chem. Phys., 20(21), 12795-12811, https://doi.org/10.5194/acp-20-12795-2020, 2020b.

Zhang, Y. X., Tao, S., Shen, H. Z., and Ma, J. M.: Inhalation exposure to ambient polycyclic aromatic hydrocarbons and lung cancer risk of Chinese population, Proc. Natl. Acad. Sci. U.S.A., 106(50), 21063-21067, https://doi.org/10.1073/pnas.0905756106, 2009.

Zhou, S., Lee, A. K. Y., McWhinney, R. D., and Abbatt, J. P. D.: Burial Effects of Organic Coatings on the Heterogeneous Reactivity of Particle-Borne Benzo a pyrene (BaP) toward Ozone, J. Phys. Chem. A, 116(26), 7050-7056, https://doi.org/10.1021/jp3030705, 2012.

Zhou, S., Shiraiwa, M., McWhinney, R. D., Poschl, U., and Abbatt, J. P.: Kinetic limitations in gas-particle reactions arising from slow diffusion in secondary organic aerosol, Faraday Discuss, 165, 391-406, https://doi.org/10.1039/C3FD00030C, 2013.